Available online at www.sciencedirect.com
ScienceDirect
JOURNAL OF IRON AND STEEL RESEARCH, INTERNATIONAL. 2012, 19(12): 42-47

Influence of Alloying Elements on Mechanical Properties and Corrosion Resistance of Cold Rolled C-Mn-Si TRIP Steels

ZHANG Ling-yun[1], WU Di[2], LI Zhuang[3]
(1. Liaoning Key Laboratory of Aircraft Digital Manufacturing and Test Technologies, Shenyang Aerospace University, Shenyang 110136, Liaoning, China; 2. State Key Laboratory of Rolling and Automation, Northeastern University, Shenyang 110004, Liaoning, China; 3. School of Materials Science and Engineering, Shenyang Aerospace University, Shenyang 110136, Liaoning, China)

Abstract: The rust layer plays an important role in the corrosion of steel in chlorinated environments. Salt spray, potentiodynamic polarization curve and tensile test were conducted in laboratory for the specimens after two-stage heat treatment. The influence of the alloying elements on mechanical properties and corrosion resistance of three kinds of steels was investigated by observing the microstructure and the morphologies of rust layer. The results show that the highest value (29%) of total elongation for steel A is obtained. The mechanical property of the specimen for steel C exhibits best strength ductility balance (21 384 MPa • %) because of the presence of the multiphase microstructures after a two-stage heat treatment and the addition of the alloying elements. The corrosion products are known to be a complex mixture of Fe_3O_4, Fe_2O_3 and α-FeOOH for steel C. The presence of the alloying elements results in the formation of compact and dense rust layers in steel B and C. Passive film protects the substrate of TRIP (transformation induced plasticity) steel containing a complex mix of multiphase. Superior corrosion performance is exhibited for steel C with low alloying contents due to the enrichment of alloying elements within the rust layers.
Key words: TRIP steel; alloying element; rust layer; mechanical property; corrosion performance

Corrosion is a worldwide problem. Marine environments corrosion of metals is the most serious one among all of corrosion[1]. Mild and low alloy steels have been widely used for many years in a variety of marine applications[2]. In marine atmospheric environments, the costs of damages associated with the corrosion of steel components are enormous.

Mild and low alloy steels are selected for their favorable combination of strength, toughness and formability. However, one of the most important factors that affect their application is the corrosion resistance. It is well known that TRIP (transformation induced plasticity) steel exhibits an excellent combination of strength and formability compared to solid solution steels and DP (dual phase) steel[3]. With a small amount of alloying elements, these steels can prevent corrosion under marine environments. It is necessary to add these costly alloying elements in order to improve corrosion resistance despite that welding characteristic might be deteriorated. There are relatively few available systematic studies about corrosion resistance of multiphase TRIP steels.

Electrochemical corrosion behavior of TRIP steel in 3.5% of NaCl solution is similar to that in actual seawater conditions. In this paper, salt spray and potentiodynamic polarization curve test were conducted in laboratory for the specimens after two-stage heat treatment. The mechanical properties and corrosion resistance of three kinds of steels were discussed by observing the microstructure and the morphologies of rust layer.

1 Experimental Procedure

1.1 Specimen preparation

Cast ingots were hot-rolled to a thickness of 4 mm, and then cold-rolled to 1 mm in thickness. The chemi-

Foundation Item: Item Sponsored by National Natural Science Foundation of China (50334010); Shenyang City Application Basic Research Project of China (1071198-1-00)
Biography: ZHANG Ling-yun(1963—), Male, Doctor, Professor; **E-mail**: zhangly79@163.com; **Received Date**: October 28, 2011

cal compositions of three kinds of steels are given in Table 1. Steel A is the conventional C-Mn-Si TRIP steel, steel B is the conventional weathering steel, and steel C is a TRIP steel with Al, Cu, Cr, Mo and Ni contents. The specimens parallel to the rolling direction were machined. These specimens were heat-treated in salt baths following the two-stage thermal cycle, as shown in Table 2.

Table 1 Chemical composition of experimental steels (mass percent, %)

Steel	C	Si	Mn	S	P	Al	Cu	Cr	Mo	Ni
A	0.111	1.230	1.380	0.013	0.009	0.180	—	—	—	—
B	0.082	0.252	0.406	0.007	0.079	0.008	0.279	0.495	—	0.310
C	0.098	1.180	1.630	0.006	0.092	0.269	0.297	0.490	0.379	0.287

Table 2 Heat treatment parameters

Specimens	Intercritical annealing	Holding	Cooling
A	810 ℃×180 s	400 ℃×300 s	Quenching in oil
B	790 ℃×180 s	400 ℃×300 s	Quenching in oil
C	780 ℃×180 s	400 ℃×300 s	Quenching in oil

Salt spray test was performed using five same specimens with size of 100 mm×50 mm×4 mm which were cut from steels A, B and C, respectively. Three same specimens with size of 15 mm×15 mm×3 mm for potentiodynamic polarization curve test were machined from each of these steels, respectively. Then these specimens were heat-treated (Table 2).

1.2 Accelerated test

The steels were exposed in the salt spray chamber at (35±2) ℃ for a period of 120 h. NaCl was provided during salt spray period, and the NaCl concentration in the chamber was controlled at (50±5) g/L. The experiment was conducted according to the standard of GB/T/10125—1997.

The polarization curves were measured at 30 ℃ with a scan rate of 10 mV/min in a solution of 3.5% of NaCl using a potentiostat and a three-electrode system consisting of saturated calomel electrode (SCE) reference electrode, Pt counter electrode and specimen.

1.3 Analytical test methods

Tensile tests were performed on an Instron 4206 machine at strain rate of 5 mm/min. The microstructures of the transverse section of the specimens after heat treatment and the morphologies of rust layers after salt spray test were observed by using light optical microscope (LOM) and scanning electron microscope (SEM), respectively. Energy dispersive spectroscopy and X-ray diffraction were used to analyse the corrosion products.

2 Experimental Results

2.1 Mechanical properties

Ultimate tensile strength R_m, yield strength R_{eL}, total elongation A_{50} and the product of ultimate tensile strength and total elongation $R_m \times A_{50}$ of three kinds of steels are presented in Table 3. It can be seen from Table 3 that A_{50} for steel A reached a maximum of 29%, and R_m for steel C reached a maximum of 973 MPa. Specimens A-1, A-2 and A-3 exhibited high value of R_m and A_{50}. The mechanical properties are low in the case of specimens B-1, B-2 and B-3. However, specimens C-1, C-2 and C-3 exhibited the highest R_m despite the presence of moderate value of A_{50}.

Table 3 Mechanical properties of specimens

Specimen number		R_m/MPa	R_{eL}/MPa	A_{50}/%	$R_m \times A_{50}$/(MPa·%)
A	A-1	508	306	28	14224
	A-2	504	303	29	14616
	A-3	511	310	27	13797
B	B-1	435	287	21	9135
	B-2	449	294	20	8980
	B-3	434	285	22	9548
C	C-1	972	655	22	21384
	C-2	969	650	22	21318
	C-3	973	657	21	20433

Fig. 1 shows the stress-strain curves from tensile test of specimens A-2, B-3 and C-1. It can be seen from Fig. 1 that yield plateau did not exist for three kinds of steels. The stress-strain curves are all characterized by low yield ratio.

2.2 Microstructures

The micrographs of the specimens after heat treatment are shown in Fig. 2. Specimens A-2, B-3 and C-1 denote the maximum combination of ultimate

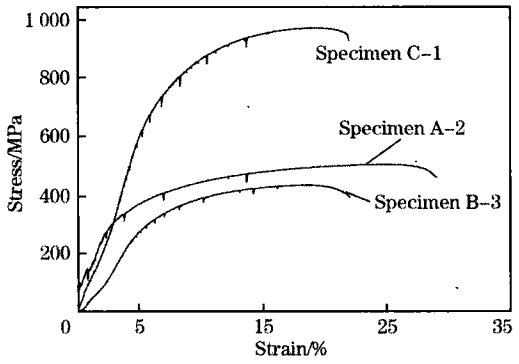

Fig. 1 Stress-strain curves of tensile test of specimens

tensile strength and total elongation for each group, respectively. In Fig. 2 (a), the micrograph consists of polygonal ferrite, granular bainite and retained austenite, and it is consistent with the results of microstructural examination presented in Ref. [4]. The pearlite and ferrite constitute the major phase of the microstructure in Fig. 2 (b). Because of the addition of alloying elements in steel C, such as Al, Cu, Cr, Mo, and Ni, etc, a multiphase microstructure consisting of the ferrite matrix with a dispersion of bainite, metastable retained austenite, and martensite is obtained, as shown in Fig. 2 (c).

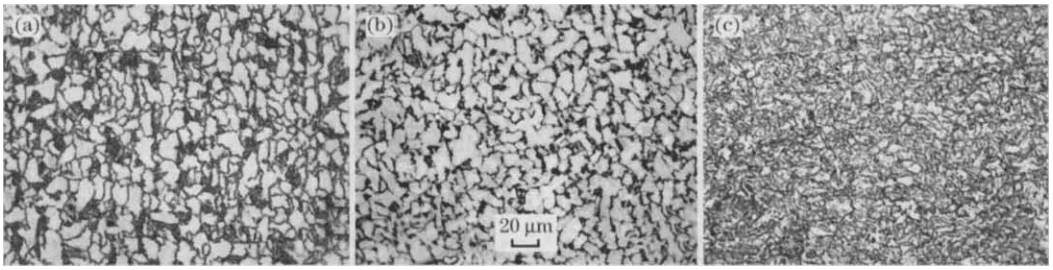

(a) Specimen A-2; (b) Specimen B-3; (c) Specimen C-1.

Fig. 2 Optical micrographs of specimens

2.3 Corrosion resistance

Fig. 3 presents the results of salt spray test. In Fig. 3, the average corrosion rates are different for three kinds of steels. The average corrosion rate of steel A reaches 0.2388 mm/a, and lower values of average corrosion rates (0.1503 and 0.1307 mm/a) of steel B and C are obtained, respectively. The corrosion performance of steel C is somewhat higher than that of steel B.

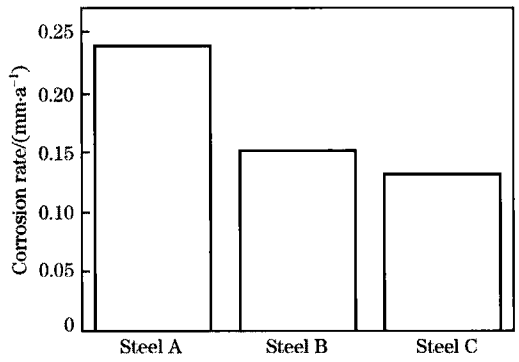

Fig. 3 Results of salt spray test

The polarization curves of three kinds of steels are shown in Fig. 4. In Fig. 4, these steels have the characteristics of surface active properties. However, the anodic current densities of steel B and C are much less than that of steel A, that is, the corrosion rate of steel A is greater than that of steel B and C. On the other hand, the corrosion rate of steel B is greater than that of steel C, that is, corrosion resistance of steel C is better than that of steel B. The result of electrochemical test is consistent with that of salt spray test.

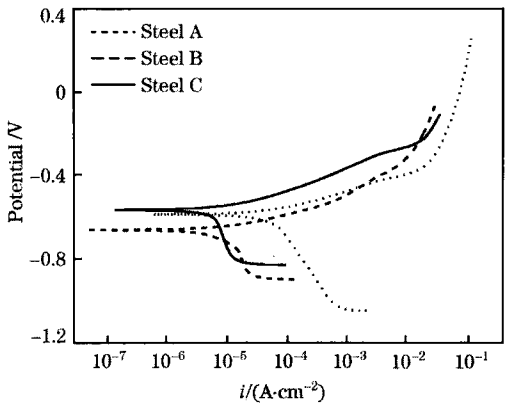

Fig. 4 Polarization curves of three kinds of steels

Fig. 5 shows the corrosion morphologies of the rust layer surfaces of three kinds of steels after the salt spray tests. The rust layers of steel B and C are compact and those of steel A are loose, and the rust layers of steel C are relatively denser compared to steel B because of the addition of aluminium and molybdenum.

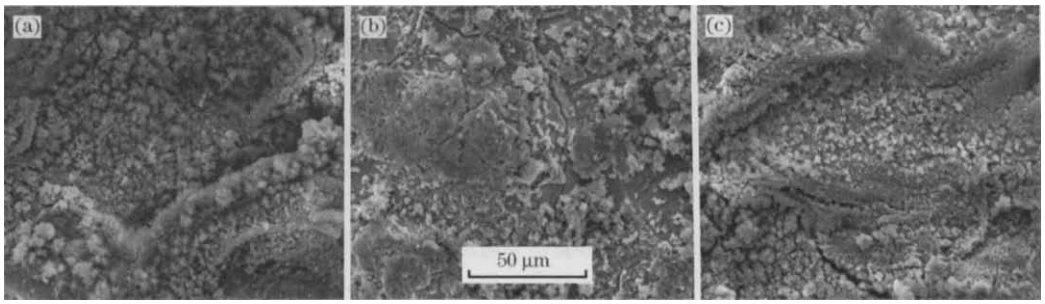

(a) Steel A; (b) Steel B; (c) Steel C.

Fig. 5 Morphologies of corrosion products of three kinds of steels after salt spray tests

Line scan maps with an energy dispersive spectrometry (EDS) microanalysis for these rust layers are shown in Fig. 6. It is apparent from Fig. 6 that the peaks appear due to the much more alloying elements in steel B and C. The alloying elements, such as Al, Cu, Cr, Mo, and Ni, etc, are especially enriched in the rust layer of steel C.

Fig. 7 shows the X-ray diffraction patterns of rust formed on steel C after salt spray test. In the case of salt spray test, the peaks of α-FeOOH were clearly observed as crystalline rust constituents. The rust layers formed on steel C were composed of

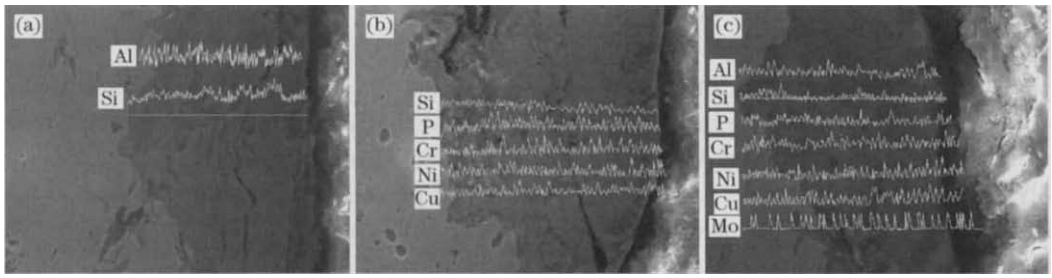

Fig. 6 Element distribution maps on rust layer of steel A (a), steel B (b) and steel C (c) after salt spray test

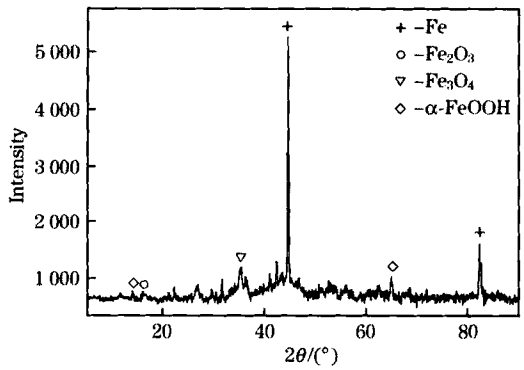

Fig. 7 XRD spectra of rust layer of steel C

Fe_3O_4, Fe_2O_3 and α-FeOOH.

3 Discussion

Good mechanical properties were obtained for conventional C-Mn-Si TRIP steel (steel A) and steel C (adding alloying elements). This is attributed to the presence of the multiphase microstructures in steel A and C after a two-stage heat treatment. Strain induced transformation to martensite of retained austenite occurs in steel A and C[4-5]. The specimens exhibited a good combination of ultimate tensile strength and total elongation.

The addition of the alloying elements plays an important role in enhancing the mechanical properties for TRIP steels. In steel A and C, additional Mn and Ni make the retained austenite content larger, Si improves the uniform elongation by increasing the stability of retained austenite, and Al increases the stability of retained austenite in much the same way as Si. Cu, Cr and Ni contribute to solid solution hardening effect in TRIP steels. Moreover, Cr and Mo have a strong solute drag effect, resulting in the improvememt of mechanical properties, and they can be considered as the addition to the conventional TRIP steel. Therefore, the highest values of tensile strength (973 MPa) for steel C, total elongation (29%) for steel A and strength ductility balance for steel A and C are obtained, respectively.

It is well known that most corrosion reactions are electrochemical in nature, and for electrochemical corrosion to occur, a cell consisting of an anode,

a cathode, an electrolyte, and a pathway for electron flow between anode and cathode is needed. Needless to say, a single-phase alloy possesses very high corrosion resistance. However, the passivation of steel is very important in the same manner. It is suggested that passive film protects the multiphase substrate for the present steels.

In particular, steel C exhibits compact rust layers, compared to steel A (Fig. 5). This is related to the addition of alloying elements in steel, such as Al, Cu, Cr, Mo, and Ni, etc[6-7]. C Keiser[8] thought that these alloying elements can retard the growth of rust, suppress the supply of oxygen to the steel surface, reduce the conductivity of the rust, precipitate and cover the steel surface, retard the crystallization of rust and contribute to a uniform dissolution of the steel.

The conduction of electricity of Cl^- ions strengthens ion access during the salt spray and polarization curve tests, which contributes to their corrosion processes. Molybdenum is dissolved as MoO_4^{2-} ions during corrosion processes, which are adsorbed on the metal surface. As a result, the penetration of Cl^- ions is suppressed[9] for the steel C containing 0.379% molybdenum. The beneficial effect of Mo addition was assigned to Mo^{6+} presence within the passive film, rendering it more stable against breakdown caused by attack of aggressive Cl^- ions, and to the formation of Mo insoluble compounds in the aggressive pit environment facilitating the pit repassivation[10]. In addition, the addition of aluminum, copper and chromium contributes to passivating for TRIP steel. Depending on protective "passivating" films, TRIP steel can inhibit further corrosion of the underlying steel.

In the present experiment, the corrosion products are known to be a complex mixture of Fe_3O_4, Fe_2O_3 and α-FeOOH. Peaks of X-ray diffraction confirm the presence of α-FeOOH for steel C. Based on the results of Zhang Q C et al[11], γ-FeOOH forms firstly and then transforms to α-FeOOH and Fe_3O_4 in the rust layer on the surface of low alloy steel. The rust layer with phase constituent of α-FeOOH has cation selective performance, and could suppress the penetration of Cl^-[12].

The presence of the alloying elements results in the formation of compact and dense rust layer in steel B and C. The aluminium and molybdenum additions to the steel C can enrich the rust-layer/substrate interface and rust layers, respectively. They can therefore enhance the compactness and densification of these rust layers. Chen Y Y et al[13] pointed out that the protective rust layer for these steels includes the inner rust layer and the outer layer, and the inner rust layer enriched with alloying elements, is compact and has a protective ability.

The rust layers on steels play an important role for corrosion progress and prevention of the substrate steels[14-16]. In the present study, the enrichment of alloying elements within the rust layer contributes to the improvement of electrochemical characteristic of TRIP steel. Therefore, smaller corrosion rates in 3.5% (mass percent) of NaCl solutions are obtained for steel C. As a result, TRIP steel containing a complex mix of multiphase with low alloying contents shows superior corrosion performance in chlorinated environments. At the same time, satisfactory mechanical properties were obtained for TRIP steel.

4 Conclusions

1) The highest value (29%) of total elongation for steel A is obtained. The mechanical property of the specimen for steel C exhibits best strength ductility balance (21384 MPa · %). This is attributed to the presence of the multiphase microstructures after a two-stage heat treatment and the addition of the alloying elements in TRIP steel.

2) Superior corrosion performance is exhibited for steel C with low alloying contents due to the compactness and densification of rust layers and the enrichment of alloying elements within the rust layer.

3) High strength TRIP steel with low alloying contents shows superior corrosion performance in chlorinated environments. Passive film protects the substrate of TRIP steel containing a complex mix of multiphase.

References:

[1] Syed S. Atmospheric Corrosion of Carbon Steel at Marine Sites in Saudi Arabia [J]. Materials and Corrosion, 2010, 61(3): 238.

[2] Osório W R, Peixoto L C, Garcia L R, et al. Electrochemical Corrosion Response of a Low Carbon Heat Treated Steel in a NaCl Solution [J]. Materials and Corrosion, 2009, 60(10): 804.

[3] Han S, Seong H, Ahn Y, et al. Effect of Alloying Elements and Coiling Temperature on the Recrystallization Behavior and the Bainitic Transformation in TRIP Steels [J]. Met Mater Int, 2009, 15(4): 521.

[4] LI Zhuang, WU Di, LÜ Hui-sheng. Effect of Thermomechanical Processing on Mechanical Properties of Hot Rolled Multiphase Steel [J]. Journal of Iron and Steel Research, International, 2008, 15(1): 55.

[5] Li Z, Wu D. Effects of Hot Deformation and Subsequent Aus-

tempering on the Mechanical Properties of Si-Mn TRIP Steels. ISIJ Int, 2006, 46(1): 121.

[6] Hsu C H, Chen M L. Corrosion Behavior of Nickel Alloyed and Austempered Ductile Irons in 3.5% Sodium Chloride [J]. Corrosion Science, 2010, 52(9): 2945.

[7] Liu C T, Wu J K. Influence of PH on the Passivation Behavior of 254SMO Stainless Steel in 3.5% NaCl Solution [J]. Corrosion Science, 2007, 49(5): 2198.

[8] Keiser J T, Brown C W, Heidersbach R H. Electrochemical Reduction of Rust Films on Weathering Steel Surfaces [J]. J Electrochem Soc, 1982, 129(12): 2686.

[9] He Y D, Qi H B. Corrosion and Protection of Material [M]. Beijing: Mechanical Industry Press, 2005.

[10] Pardo A, Merino M C, Coy A E, et al. Pitting Corrosion Behaviour of Austenitic Stainless Steels-Combining Effects of Mn and Mo Additions [J]. Corrosion Science, 2008, 50(6): 1796.

[11] Zhang Q C, Ma F, Wu J S, et al. Mechanical Properties of Native Rust Layer Formed on a Low Alloy Steel Exposed in Marine Atmosphere [J]. ISIJ Int, 2002, 42(5): 534.

[12] Miyuki H, Yamashita M, Fujiwara M, et al. Ion Selective Properties of Rust Membranes and Protective Effect of Stable Rust Layer Formed on Weathering Steel [J]. Zairyo to Kankyo/Corrosion Engineering, 1998, 47(3): 186.

[13] Chen Y Y, Tzeng H J, Wei L I, et al. Mechanical Properties and Corrosion Resistance of Low-Alloy Steels in Atmospheric Conditions Containing Chloride [J]. Materials Science and Engineering, 2005, 398A: 47.

[14] Toshiaki O, Tomohiro K. Enhancement of Electric Conductivity of the Rust Layer by Adsorption of Water [J]. Corrosion Science, 2005, 47(10): 2571.

[15] Corvo F, Perez T, Dzib L R, et al. Outdoor-Indoor Corrosion of Metals in Tropical Coastal Atmospheres [J]. Corrosion Science, 2008, 50(1): 220.

[16] Tamura H. The Role of Rusts in Corrosion and Corrosion Protection of Iron and Steel [J]. Corrosion Science, 2008, 50 (7): 1872.